

Article

Exploring the Validity of Plane and Spherical Millimeter-Wave Incidences for Multiple-Diffraction Calculations in Wireless Communication Systems

Alba López-Segovia ¹, Ignacio Rodríguez-Rodríguez ², José-Víctor Rodríguez ^{1,*}, Leandro Juan-Llácer ¹,
María Campo-Valera ¹ and Wai Lok Woo ³

¹ Departamento de Tecnologías de la Información y las Comunicaciones, Universidad Politécnica de Cartagena, Antiguo Cuartel de Antigones, Plaza del Hospital, 1, Cartagena, 30202 Murcia, Spain

² Departamento de Ingeniería de Comunicaciones, Universidad de Málaga, Avda. Cervantes, 2, 29071 Málaga, Spain

³ Department of Computer and Information Sciences, Northumbria University, Newcastle upon Tyne NE1 8ST, UK; wailok.woo@northumbria.ac.uk

* Correspondence: jvictor.rodriguez@upct.es; Tel.: +34-968-326-548

Abstract: The focus of this work is to determine at which threshold can the results for both plane and spherical wave incidence assumptions either converge or deviate when performing multiple diffraction attenuation calculations. The analysis has been carried out—for various millimeter-wave frequencies, inter-obstacle spacings, and angles of incidence—by employing a pair of two-dimensional (2D) hybrid formulations based on both the uniform theory of diffraction and physical optics (UTD-PO). This way, we seek to demonstrate under which circumstances each wave incidence assumption can be valid in environments that entail millimeter-wave bands. Based on this, we may ensure the minimum necessary distance from the transmitter to the first diffracting obstacle for the convergence of the spherical wave incidence solution onto that of the plane wave with a relative error below 0.1%. Our results demonstrate that for less than four diffracting elements, the minimum necessary distance engages in quasi-linear behavior under variations in both the angle of incidence and obstacle spacing. Notably, the considered frequencies (60–100 GHz) have almost no bearing on the results. Our findings will facilitate the simplified, more accurate and realistic planning of millimeter-wave radio communication systems, with multiple diffractions across various obstacles.

Keywords: radio communication systems; multiple diffraction; millimeter-wave frequency band; uniform theory of diffraction



Citation: López-Segovia, A.; Rodríguez-Rodríguez, I.; Rodríguez, J.-V.; Juan-Llácer, L.; Campo-Valera, M.; Woo, W.L. Exploring the Validity of Plane and Spherical Millimeter-Wave Incidences for Multiple-Diffraction Calculations in Wireless Communication Systems. *Electronics* **2023**, *12*, 2020. <https://doi.org/10.3390/electronics12092020>

Academic Editors: Syed Muzahir Abbas, Yang Yang and Adão Silva

Received: 6 March 2023

Revised: 25 April 2023

Accepted: 26 April 2023

Published: 27 April 2023



Copyright: © 2023 by the authors. Licensee MDPI, Basel, Switzerland. This article is an open access article distributed under the terms and conditions of the Creative Commons Attribution (CC BY) license (<https://creativecommons.org/licenses/by/4.0/>).

1. Introduction

The analysis of the multiple diffraction experienced by radio waves due to the presence of obstacles in their propagation path has been extensively studied through numerous formulations. These solutions are usually based on the uniform theory of diffraction (UTD) [1,2], physical optics (PO) [3,4], or both theories [5,6], and aim to predict the losses caused by this phenomenon by modeling the mentioned obstacles as knife-edges and assuming a plane wave incidence over them in most cases. In this case, when the number of these obstacles is large, the multiply diffracted field is approximated by the so-called *Q* factor, as proposed in [3].

However, in micro/picocellular environments where the transmitting antenna may be located at a short distance from the series of diffracting elements, the assumption of a plane wave incidence on them may not yield realistic results. Therefore, in such a case, considering a spherical wave incidence could be more appropriate in terms of obtaining predictions of losses due to multiple diffraction that are more in line with reality.

On the other hand, future wireless telecommunication systems are required to offer higher data rates and capacity to cope with the next generation of high-bandwidth

multimedia services. In this context, frequency bands located between 60 and 100 GHz have captured the interest of researchers due to the large available bandwidth [7] and the small frequency reuse distance it offers [8], which allows for the development of low-range indoor systems with low-power transmitters, but with transmission rates of up to several gigabits per second [9].

Regarding the above, numerous papers have been published on radio wave propagation models at millimeter frequencies [10–14], and specifically, several works have addressed the analysis of multiple diffraction at such frequencies [15–17]. However, none of the previous work addresses the fact of checking beforehand, whether the distance between the transmitter and the first obstacle is large enough for a plane-wave incidence assumption to be valid, which could lead to inaccurate or unrealistic results. On the other hand, it is also not verified if when a spherical-wave incidence is being considered, a plane-wave assumption could be perfectly used instead, with the improvement in terms of computational efficiency that this would entail.

In this work, in order to clarify the distance range between the transmitter and the first diffracting element in which each type of incidence would be valid, a comparison of the losses due to multiple diffractions caused by a series of obstacles for both plane and spherical-wave assumptions is presented, while considering a range of frequencies between 60 and 100 GHz, as well as several angles of incidence and spacing between diffracting elements. The analysis is carried out using two hybrid UTD-PO formulations (for plane and spherical-wave incidences, respectively) developed by the authors [5,6], which are more computationally efficient than other existing solutions. Moreover, the study considers an environment in which millimeter-wave communication systems are being used, and attenuation due to multiple diffraction needs to be calculated over a series of objects. In other words, the main novelty of the paper is the calculation of the limits at which both UTD-PO multiple-diffraction formulations—based on two different wave-incidence assumptions (plane and spherical)—converge or differ, at millimeter-wave frequencies. In this sense, the results will establish the validity of both types of incidence depending on the distance between the transmitter and the first diffracting obstacle, thereby alerting about an improper use of one or the other formulation, which may lead to inaccurate or computationally demanding results.

2. Propagation Environment

Figure 1 shows a diagram of the propagation environment considered, where n obstacles are modeled as parallel and absorbent edges, separated by a constant distance w and at the same height H relative to the transmitter T_x . Additionally, the transmitter is assumed to be located above the height of the obstacles and at a distance d from the first obstacle. Furthermore, the reference point where the received field will be obtained is assumed to be located at a distance w from the last obstacle considered.

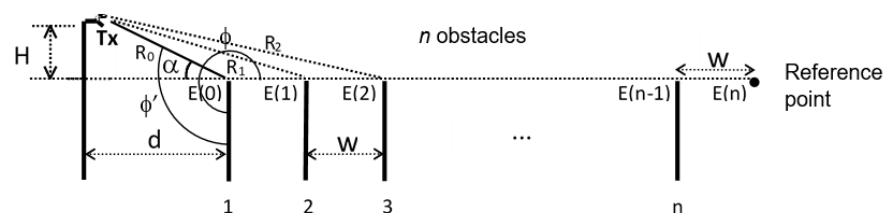


Figure 1. Scheme of the considered propagation environment.

3. Theoretical Models

The following theoretical models are described to evaluate multiple diffraction in both the case of a plane wave incident on the obstacles and a spherical wave.

3.1. Plane Wave Incidence

For $n = 1$, considering UTD, the field that reaches the reference point in Figure 1 can be calculated as:

$$E(1) = E(0) \left[\exp(-jk\omega \cos \alpha) + \frac{1}{\sqrt{w}} D(\varphi = \frac{3\pi}{2}, \varphi' = \frac{\pi}{2} + \alpha, L = w) \exp(-jk\omega) \right] \quad (1)$$

where $E(0) = E_0$ (being that E_0 is the amplitude of the transmitted plane wave, which is assumed to be 1), k is the wave number, and $D(\varphi, \varphi', L)$ is the diffraction coefficient for an absorbent knife-edge proposed in [18] (φ is the angle between the diffracting obstacle and the incident ray, φ' is the angle between the diffracting obstacle and the diffracted ray, and L is a distance parameter, as can be observed in Figure 1).

For $n = 2$, multiple diffraction arises, and following the same PO recursive procedure as that presented by Saunders and Bonar in [4], the field at the reference point in Figure 1 can be obtained as the average of two contributions expressed in terms of UTD single diffractions:

$$E(2) = \frac{1}{2} \left[\begin{aligned} &E(0) \left[\exp(-jk2\omega \cos \alpha) + \frac{1}{\sqrt{2w}} D(\varphi = \frac{3\pi}{2}, \varphi' = \frac{\pi}{2} + \alpha, L = 2w) \exp(-jk2\omega) \right] \\ &+ E(1) \left[\exp(-jk\omega \cos \alpha) + \frac{1}{\sqrt{w}} D(\varphi = \frac{3\pi}{2}, \varphi' = \frac{\pi}{2} + \alpha, L = w) \exp(-jk\omega) \right] \end{aligned} \right] \quad (2)$$

Therefore, if the previous process is generalized for n knife-edges—by considering the hybrid UTD-PO methodology presented in [5] for the analysis of multiple diffraction of plane waves—the total field that reaches the reference point in Figure 1 can be expressed, assuming $d \gg nw$ and for $n \geq 1$ as:

$$E(n) = \frac{1}{n} \sum_{m=0}^{n-1} E(m) \{ \exp[-jk(n-m)\omega \cos \alpha] + \frac{1}{\sqrt{(n-m)w}} D(\varphi = \frac{3\pi}{2}, \varphi' = \frac{\pi}{2} + \alpha, L = (n-m)w) \exp[-jk(n-m)\omega] \} \quad (3)$$

The main advantage of this formulation is that, due to its recursion, the calculations of each iteration are expressed in terms of single diffractions, thus avoiding the consideration of higher order terms in the diffraction coefficients (*slope* diffraction). In this way, a simpler solution is obtained from the mathematical point of view, and therefore becomes computationally more efficient, without this fact entailing a loss of precision.

3.2. Spherical Wave Incidence

In this case, for $n = 1$ and by applying UTD, the field that reaches the reference point in Figure 1 can be calculated as:

$$\begin{aligned} E(1) &= \frac{E_0}{R_1} \exp(-jkR_1) + \frac{E_0}{R_0} \exp(-jkR_0) \sqrt{\frac{R_0}{w(R_0+w)}} D_1 \left(\varphi = \frac{3\pi}{2}, \varphi' = \frac{\pi}{2} + \alpha, L = \frac{R_0 w}{R_0+w} \right) \exp(-jk\omega) \\ &= E(0) \left(\frac{R_0}{R_1} \exp(-jk(R_1 - R_0)) + \sqrt{\frac{R_0}{w(R_0+w)}} D_1 \left(\varphi = \frac{3\pi}{2}, \varphi' = \frac{\pi}{2} + \alpha, L = \frac{R_0 w}{R_0+w} \right) \exp(-jk\omega) \right) \end{aligned} \quad (4)$$

where

$$E(0) = \frac{E_0}{R_0} \exp(-jkR_0) \quad (5)$$

with E_0 being the relative amplitude of the spherical source, which is assumed to be 1, k is the wave number, $D(\varphi, \varphi', L)$ is again the diffraction coefficient for an absorbent knife-edge proposed in [18], and R_0, R_1 are the distances that can be observed in Figure 1.

For $n = 2$, multiple diffraction emerges, and following the same methodology—based on virtual spherical sources—as presented in [6] (which, in turn, is based on the PO recursivity proposed in [4,5]), in the plane-wave case, the field at the reference point in Figure 1 can be calculated as the average of two contributions expressed in terms of UTD single diffractions:

$$E(2) = \frac{1}{2} \left[\begin{aligned} &E(0) \left(\frac{R_0}{R_2} \exp(-jk(R_2 - R_0)) + \sqrt{\frac{R_0}{2w(R_0+2w)}} D_1 \left(\varphi = \frac{3\pi}{2}, \varphi' = \frac{\pi}{2} + \alpha, L = \frac{R_0 2w}{R_0+2w} \right) \exp(-jk2\omega) \right) \\ &+ E(1) \left(\frac{R_0}{R_1} \exp(-jk(R_2 - R_1)) + \sqrt{\frac{R_0}{w(R_0+w)}} D_2 \left(\varphi = \frac{3\pi}{2}, \varphi' = \frac{\pi}{2} + \alpha, L = \frac{R_0 w}{R_0+w} \right) \exp(-jk\omega) \right) \end{aligned} \right] \quad (6)$$

Regarding the above, if we generalize the previous process for the case of n knife-edges, the total field existing at the reference point indicated in Figure 1, for $n \geq 1$, can be evaluated—by considering the UTD-PO recursive procedure presented in [6] for the analysis of losses due to multiple diffraction when the incident wavefront is spherical—as:

$$E(n) = \frac{1}{n} \sum_{m=0}^{n-1} E(m) \cdot \left[\frac{R_0}{R_{n-m}} \exp(-jk(R_n - R_m)) + \sqrt{\frac{R_0}{(n-m)w[R_0+(n-m)w]}} \cdot D\left(\varphi = \frac{3\pi}{2}, \varphi' = \frac{\pi}{2} + \alpha, L = \frac{R_0(n-m)w}{R_0+(n-m)w}\right) \cdot \exp(-jk(n-m)w) \right] \quad (7)$$

where

$$R_x = \sqrt{H^2 + (d + x \cdot w)^2} \quad (8)$$

being that, as can be observed in Figure 1, x represents the number of the considered incident ray and it can take values from 0 to $n - 1$.

Again, we obtain a recursive solution, which is also being expressed in terms of UTD single diffractions and does not need higher order terms in the diffraction coefficients, thus proving to be computationally more efficient.

4. Results

4.1. Comparison between Plane and Spherical-Wave Incidences

In Figures 2 and 3, the variation of the total field at the reference point with respect to the free-space field (attenuation in dB), is presented for the two types of wave incidence as a function of the distance of the transmitting point T_x to the first obstacle (d). A frequency of $f = 80$ GHz, $w = 0.5$ m, and two values of n (5 and 50, respectively) have been considered, as well as three values of α (1.0° , 1.75° , and 2.5° , where H varies accordingly with d in the case of spherical wave incidence to maintain these angles). It should be noted that in the case of plane wave incidence, the attenuation is independent of d , since it has been assumed that $d \gg n \cdot w$. Therefore, in that case, the results appear constant with d .

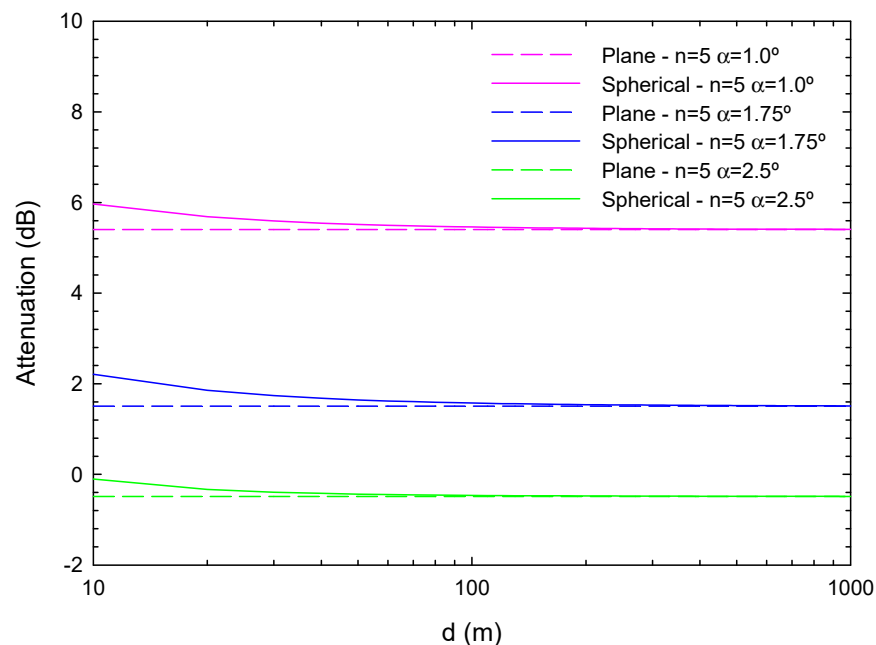


Figure 2. Variation of the total field at the reference point relative to the field in free space (attenuation), for the two types of wave incidence, as a function of the distance from the transmitting antenna to the first obstacle (d). A frequency of $f = 80$ GHz, $w = 0.5$ m, $n = 5$ and various values of α (1, 1.75, and 2.5°) have been considered.

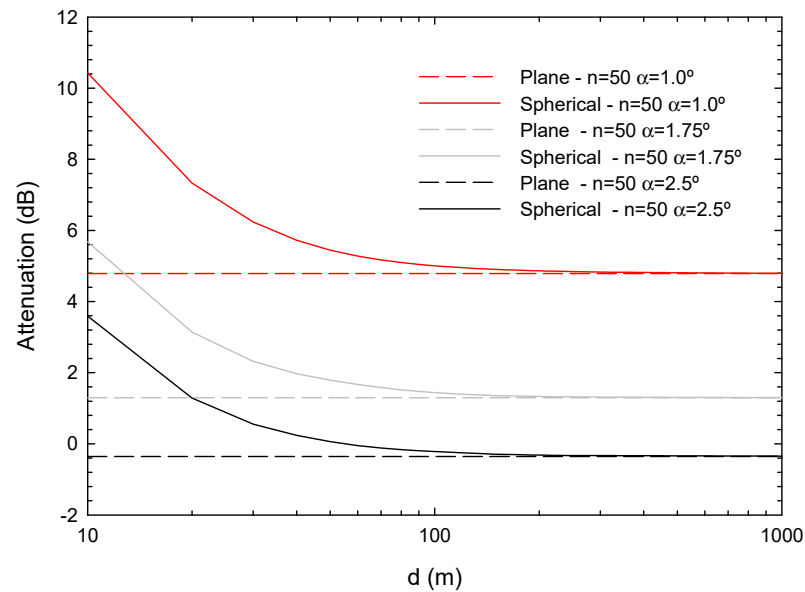


Figure 3. Variation of the total field at the reference point relative to the field in free space (attenuation), for the two types of wave incidence, as a function of the distance from the transmitting antenna to the first obstacle (d). A frequency of $f = 80$ GHz, $w = 0.5$ m, $n = 50$ and various values of α (1, 1.75, and 2.5°) have been considered.

It can be observed how the difference between the results of both solutions becomes more significant as d takes a lower value, and on the contrary, the two formulations converge for high values of d , as expected. Moreover, it is worth noting that the attenuation values for $f = 60$ GHz are the highest of the three frequencies considered—for both $n = 5$ and $n = 50$ —due to the strong absorption of radiation that occurs in the atmosphere at that frequency. On the other hand, in Figure 4, the relative error (in %) between the results of the two types of wave incidence has been represented and understood as:

$$Relative\ error = \frac{Atten.Spherical\ Wave - Atten.Plane\ Wave}{Atten.Plane\ Wave} \tag{9}$$

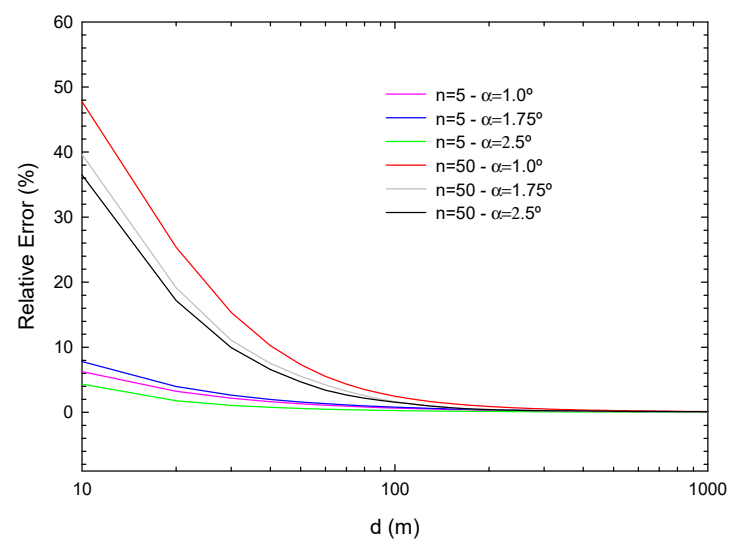


Figure 4. Relative error between the results of Figures 2 and 3 for both types of wave incidence.

From Figure 4, we can conclude that if values of d are considered increasingly, a point is reached where the relative error between both types of wave incidence becomes lower

than a certain percentage (attenuation results for plane and spherical waves converge). Therefore, for distances shorter than these values of d , considering the parameters of the scenario under study, the spherical wave solution should be assumed in order to obtain more realistic predictions of multiple diffraction attenuation, since otherwise (using the plane wave formulation) errors of up to more than 5.6 dB (for $d = 10$ m, $n = 50$, and $\alpha = 1.0^\circ$) could be reached.

In Figures 5–7, the same analysis as before is carried out (attenuation and relative error, respectively) but in this case, the parameters of $f = 80$ GHz and $\alpha = 1.5^\circ$ are fixed, and w is varied taking values of 0.1, 0.5, and 1.0 m (also for $n = 5$ and $n = 50$).

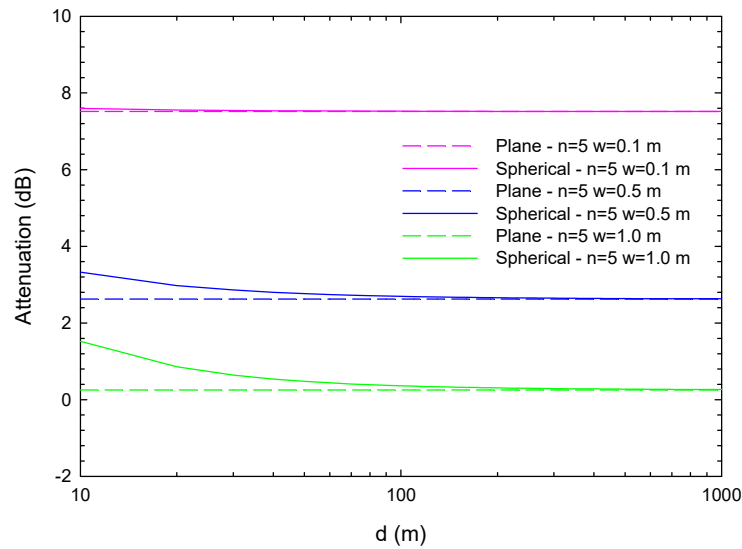


Figure 5. Variation of the total field at the reference point with respect to the free-space field (attenuation), for the two types of wave incidence, is shown as a function of the distance between the transmitting antenna and the first obstacle (d). The frequency considered is $f = 80$ GHz, the angle of incidence is $\alpha = 1.5^\circ$. $n = 5$, and several values of w (0.1, 0.5 and 1.0 m) have been taken into account.

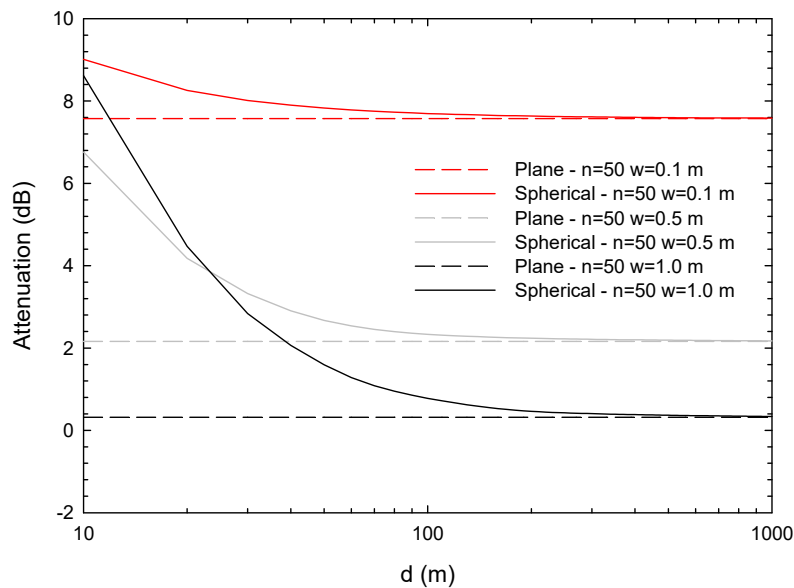


Figure 6. Variation of the total field at the reference point with respect to the free-space field (attenuation), for the two types of wave incidence, is shown as a function of the distance between the transmitting antenna and the first obstacle (d). The frequency considered is $f = 80$ GHz, the angle of incidence is $\alpha = 1.5^\circ$. $n = 50$, and several values of w (0.1, 0.5 and 1.0 m) have been taken into account.

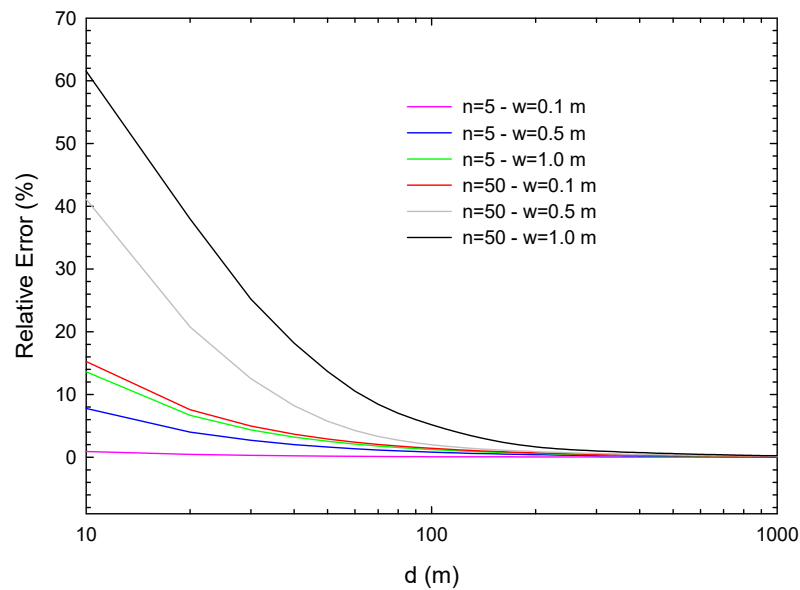


Figure 7. Relative error between the results of Figures 5 and 6 for the two types of wave incidence.

Again, the convergence of the spherical wave solution to the plane wave solution is observed, and values of d are considered larger, thus reducing the relative error between both types of incidence. On the other hand, the maximum difference between both solutions is obtained for $d = 10$, $n = 50$, and $w = 1.0$ m with 8.3 dB.

Finally, in Figures 8–10, the results of attenuation and relative error, assuming $\alpha = 1.5^\circ$, $w = 0.5$ m, $n = 5$, and 50, are shown with three different millimeter-wave frequencies (60, 80, and 100 GHz), yielding identical considerations. In this case, the maximum difference between the two formulations is obtained for $d = 10$, $n = 50$, and $f = 60$ GHz with 5.0 dB.

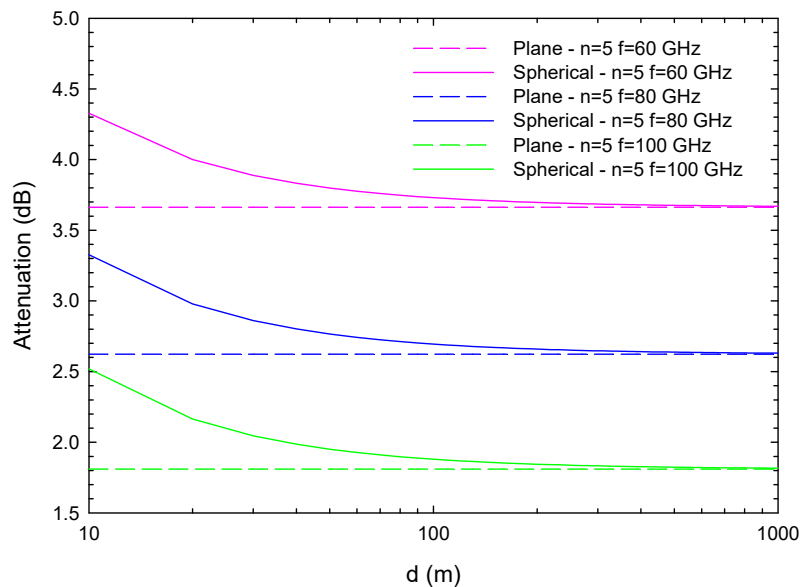


Figure 8. Variation of the total field at the reference point with respect to the free space field (attenuation) for the two types of wave incidence is shown as a function of the distance between the transmitting antenna and the first obstacle (d). The values of $n = 5$ and f (60, 80 and 100 GHz) have been considered, with $w = 0.5$ m and $\alpha = 1.5^\circ$.

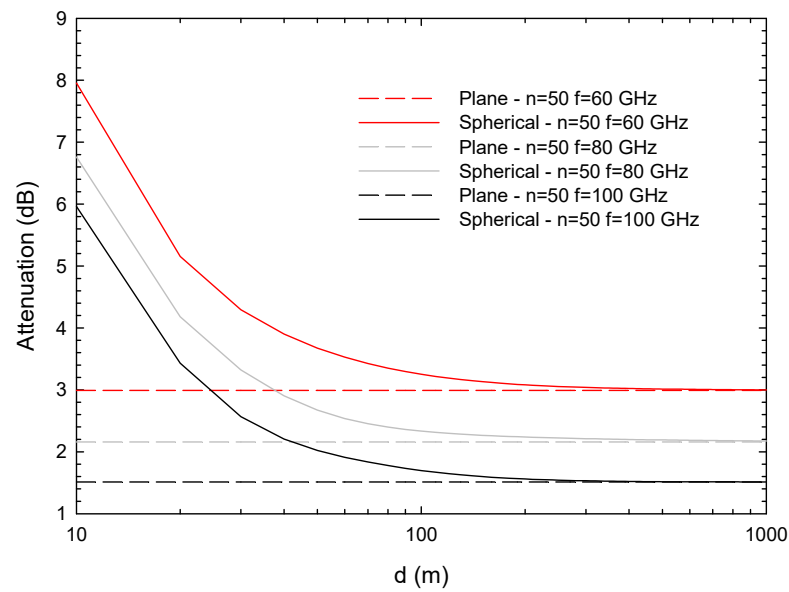


Figure 9. Variation of the total field at the reference point with respect to the free space field (attenuation), for the two types of wave incidence, is shown as a function of the distance between the transmitting antenna and the first obstacle (d). The values of $n = 50$ and f (60, 80 and 100 GHz) have been considered, with $w = 0.5$ m and $\alpha = 1.5^\circ$.

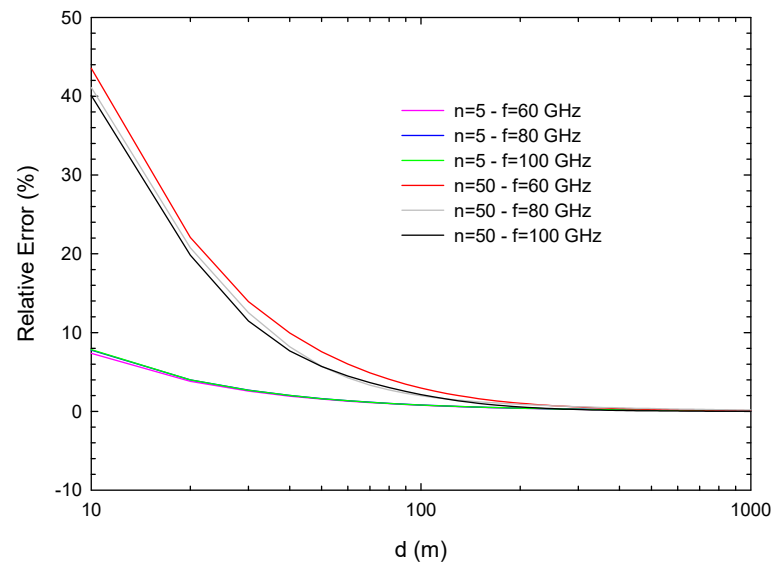


Figure 10. Relative error between the results of Figures 8 and 9 for the two types of wave incidence.

4.2. Minimum Values of d for the Two Types of Incidence to Converge

In order to delve deeper into the previous analysis, a study is presented below on the minimum values of d required for the two solutions (plane wave and spherical wave) to converge with a relative error less than 0.1%. These results are shown as a function of the incidence angle α (Figure 11, for $f = 80$ GHz and $w = 0.5$ m) and the spacing between obstacles w (Figure 12, for $f = 80$ GHz and $\alpha = 1.5^\circ$). In this sense, considering the context of wireless communication systems operating at millimeter-wave frequencies, the aforementioned study has been conducted for a small number of obstacles ($n = 1, 2, 3,$ and 4), since it is expected that in the propagation environments where these systems operate, the signal passes through few diffracting elements on its path from the transmitter to the receiver (due to the small cell size or the consideration of indoor contexts [15]).

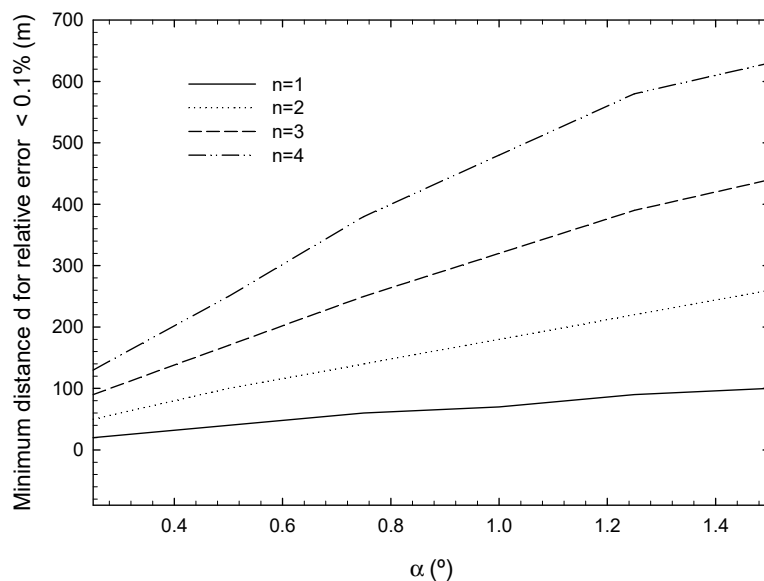


Figure 11. Minimum distance d for which the relative error between the two types of wave incidence (plane and spherical wave) is less than 0.1%, as a function of the incidence angle α and for $n = 1, 2, 3,$ and 4 ($f = 80$ GHz and $w = 0.5$ m).

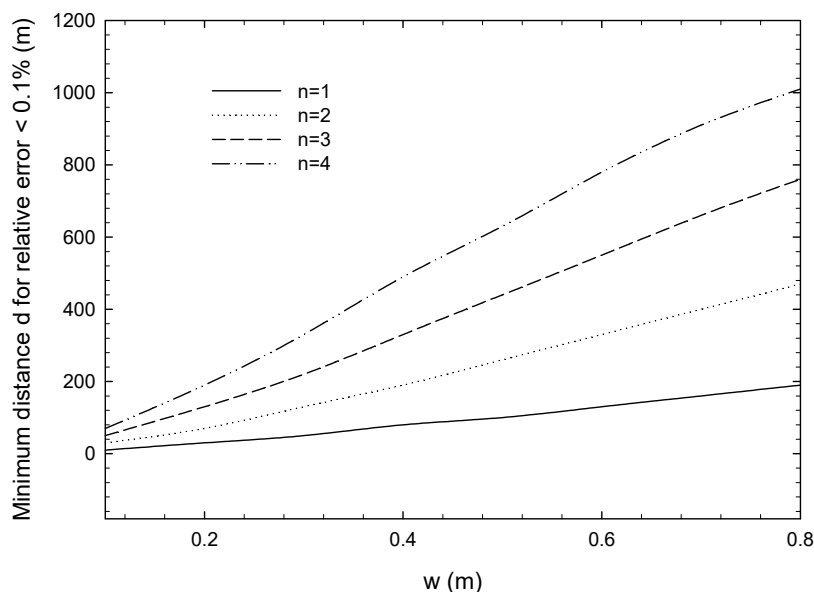


Figure 12. Minimum distance d at which the relative error between the two types of wave incidence (plane and spherical wave) is less than 0.1%, as a function of the spacing between obstacles w , for $n = 1, 2, 3$ and 4 ($f = 80$ GHz and $\alpha = 1.5^\circ$).

As can be observed, a quasi-linear behavior of the curves is apparent in both figures, with minimum values of d for relative errors $< 0.1\%$ ranging from 20 to 630 m in the case of Figure 11 (for $[n = 1, \alpha = 0.25^\circ]$ and $[n = 4, \alpha = 1.5^\circ]$, respectively), and between 10 and 1010 m in Figure 12 (for $[n = 1, w = 0.1$ m] and $[n = 4, w = 0.8$ m], respectively).

On the other hand, in order to perform an analysis of the minimum d for relative error $< 0.1\%$ as a function of frequency, Figures 13 and 14 are presented, where several incidence angles α ($0.5, 1.0,$ and 1.5° , with $w = 0.5$) and several spacing values w ($0.3, 0.5,$ and 0.7 m, with $\alpha = 1.5^\circ$) have been considered, respectively.

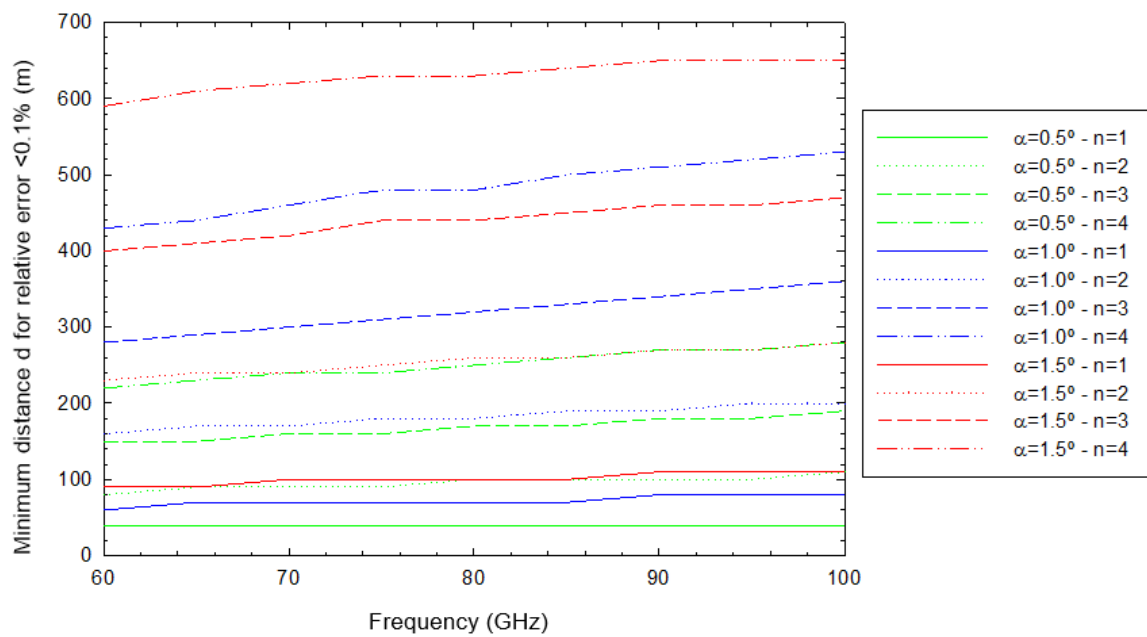


Figure 13. Minimum distance d for which the relative error between the two types of wave incidence (plane and spherical) is less than 0.1%, as a function of frequency for several values of α (0.5, 1.0, and 1.5°) and $n = 1, 2, 3,$ and 4 ($w = 0.5$ m).

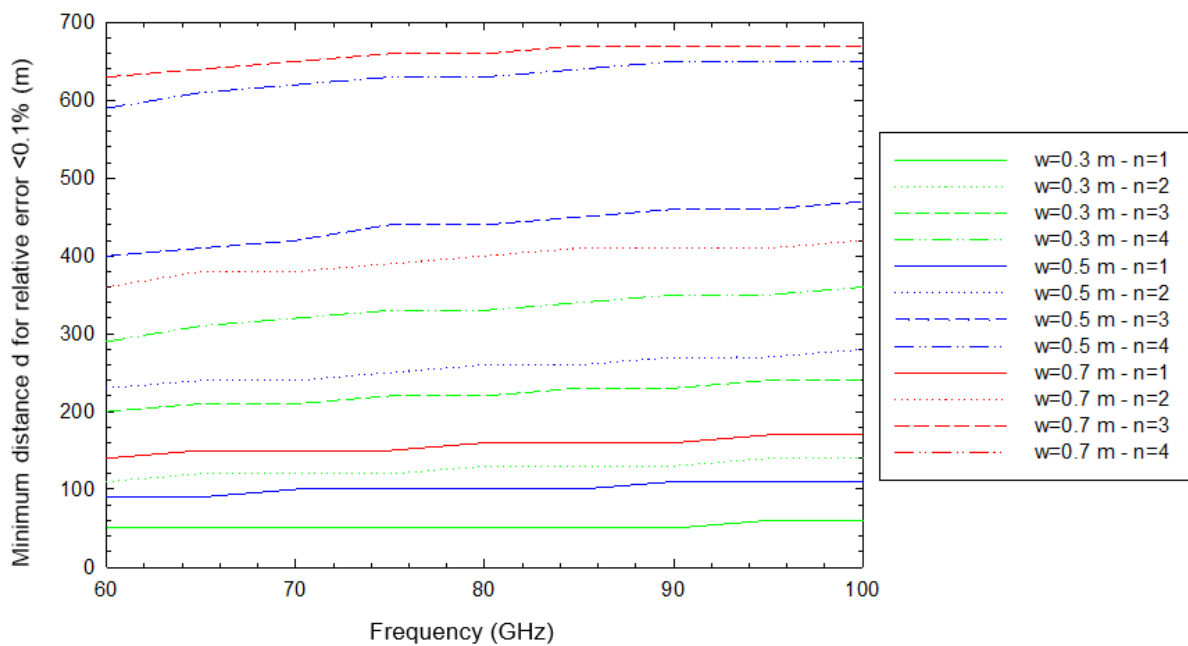


Figure 14. Minimum distance d for which the relative error between the two types of wave incidence (plane and spherical wave) is less than 0.1%, is studied as a function of frequency for several values of w (0.3, 0.5 and 0.7 m) and $n = 1, 2, 3$ and 4, considering an angle of incidence of $\alpha = 1.5^\circ$.

These two figures show a very interesting fact, since, as can be observed in both graphs, the curves practically show a constant behavior, so it can be inferred that, for a small number of obstacles (up to $n = 4$) and the considered parameters, the minimum distance d for a relative error between the two types of incidence is less than 0.1%, and can be assumed to be independent of frequency (in a range of 60 to 100 GHz).

Therefore, Figures 15 and 16 represent the minimum d for relative error $< 0.1\%$ considering different values of α (0.5, 1.0, and 1.5°, with $w = 0.5$ m) and w (0.3, 0.5, and 0.7 m, with

$\alpha = 1.5^\circ$), respectively, as a function of the number of obstacles n (from 1 to 4). Notably, considering the previous result, both figures can be perfectly valid for any millimeter-wave frequency between 60 and 100 GHz (for each given n and α/w , the average of the minimum d for relative error $< 0.1\%$ throughout the evaluated frequency range has been considered, since the variation with this last parameter has been found to be minimal). As can be observed, the behavior of the curves in both figures is quasi-linear.

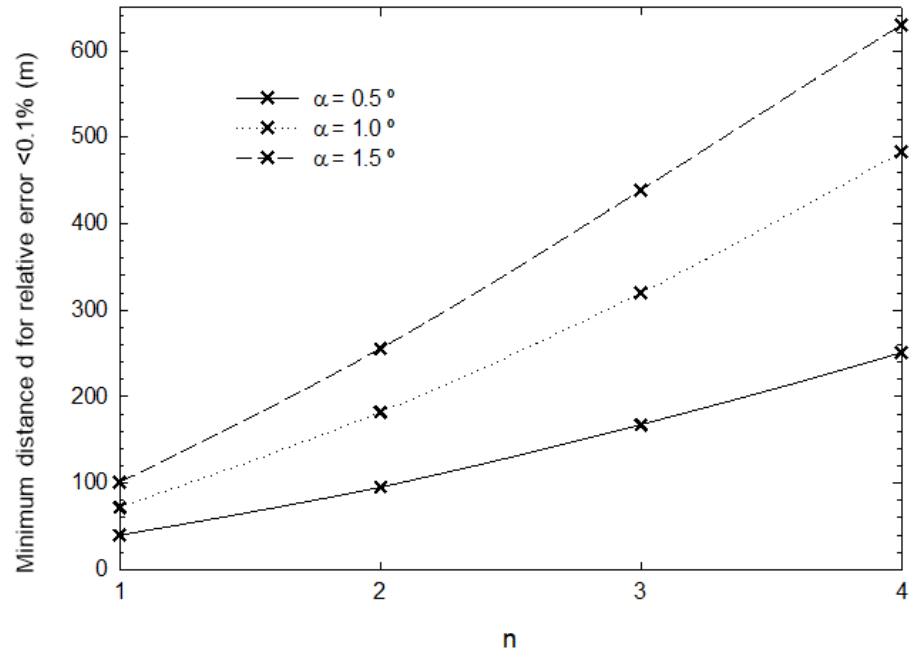


Figure 15. Minimum distance d for which the relative error between the two types of wave incidence (plane and spherical wave) is less than 0.1%, as a function of n for various values of α (0.5, 1 and 1.5°) is considered ($w = 0.5$ m).

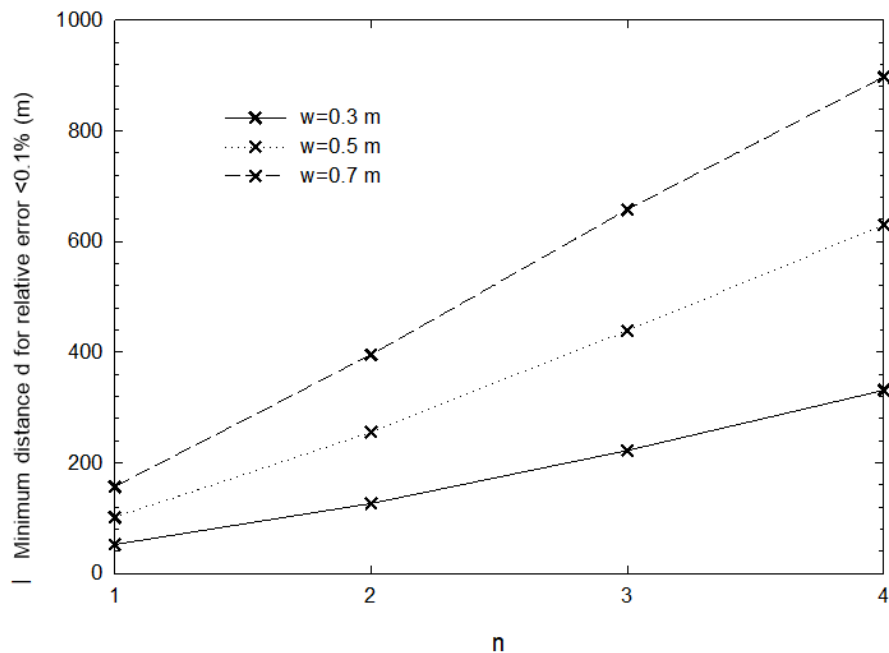


Figure 16. Minimum distance d for which the relative error between the two types of wave incidence (plane and spherical wave) is less than 0.1%, as a function of n for various values of w (0.3, 0.5 and 0.7 m) with $\alpha = 1.5^\circ$.

5. Conclusions

This work has determined at which threshold will the results for both plane and spherical wave incidence assumptions converge or deviate when performing multiple diffraction attenuation calculations. The analysis has been carried out—for various millimeter-wave frequencies, inter-obstacle spacings, and angles of incidence—by employing a pair of two-dimensional (2D) hybrid formulations based on both the uniform theory of diffraction and physical optics (UTD-PO). This way, we have calculated the minimum necessary distance from the transmitter to the first diffracting obstacle for the convergence of the spherical wave incidence solution onto that of the plane wave with a relative error below 0.1%. Our results have demonstrated that using a plane wave solution in environments where the distance between the transmitter and the first obstacle is not large enough for the spherical wave results to converge to those of the plane wave, can lead to errors in the estimation of multiple diffraction losses of more than 8 dB. Moreover, it has been demonstrated that for a few (less than four) diffracting elements, the minimum necessary distance engages in quasi-linear behavior, under variations in both the angle of incidence and obstacle spacing. Furthermore, it is interesting to note that these distance values have turned out to be practically independent of the considered millimeter-wave frequencies (60–100 GHz). The results presented in this study may contribute to a more precise and realistic planning of wireless communication systems employing millimeter wave frequencies and needing to account for the losses caused by multiple diffraction due to a series of obstacles.

Author Contributions: Conceptualization, A.L.-S., I.R.-R. and J.-V.R.; methodology, A.L.-S., I.R.-R. and J.-V.R.; software, A.L.-S., I.R.-R. and J.-V.R.; validation, A.L.-S., I.R.-R., J.-V.R., L.J.-L., M.C.-V. and W.L.W.; formal analysis, A.L.-S., I.R.-R. and J.-V.R.; investigation, A.L.-S., I.R.-R. and J.-V.R.; resources, A.L.-S., I.R.-R., J.-V.R., L.J.-L., M.C.-V. and W.L.W.; data curation, A.L.-S., I.R.-R., J.-V.R., L.J.-L., M.C.-V. and W.L.W.; writing—original draft preparation, A.L.-S., I.R.-R. and J.-V.R.; writing—review and editing, A.L.-S., I.R.-R., J.-V.R., L.J.-L., M.C.-V. and W.L.W.; visualization, A.L.-S., I.R.-R., J.-V.R., L.J.-L., M.C.-V. and W.L.W.; supervision, A.L.-S., I.R.-R., J.-V.R., L.J.-L., M.C.-V. and W.L.W.; project administration, I.R.-R., J.-V.R. and L.J.-L.; funding acquisition, I.R.-R., J.-V.R. and L.J.-L. All authors have read and agreed to the published version of the manuscript.

Funding: This work was supported by the Ministerio de Ciencia e Innovación, Spain, under Grant PID2019-107885GB-C33.

Data Availability Statement: Not applicable.

Acknowledgments: Ignacio Rodríguez-Rodríguez would like to thank Plan Andaluz de Investigación, Desarrollo e Innovación (PAIDI), Junta de Andalucía, Spain. María Campo-Valera is grateful for postdoctoral program Margarita Salas—Spanish Ministry of Universities (financed by European Union—NextGenerationEU).

Conflicts of Interest: The authors declare no conflict of interest.

References

1. Zhang, W.; Lähteenmäki, J.; Vainikainen, P. A practical aspect of over-rooftop multiple-building forward diffraction from a low source. *IEEE Trans. Electromagn. Compat.* **1999**, *41*, 115–119. [[CrossRef](#)]
2. Neve, M.J.; Rowe, G.B. Contributions towards the development of a UTD-based model for cellular radio propagation prediction. *IEE Proc. Microw. Antennas Propag.* **1994**, *141*, 407–414. [[CrossRef](#)]
3. Walfisch, J.; Bertoni, H. A theoretical model of UHF propagation in urban environments. *IEEE Trans. Antennas Propag.* **1988**, *36*, 1788–1796. [[CrossRef](#)]
4. Saunders, S.; Bonar, F. Prediction of mobile radio wave propagation over buildings of irregular heights and spacings. *IEEE Trans. Antennas Propag.* **1994**, *42*, 137–144. [[CrossRef](#)]
5. Juan-Llácer, L.; Cardona, N. UTD solution for the multiple building diffraction attenuation function for mobile radiowave propagation. *Electron. Lett.* **1997**, *33*, 92–93. [[CrossRef](#)]
6. Rodríguez, J.-V.; Molina-García-Pardo, J.-M.; Juan-Llácer, L. A new solution expressed in terms of UTD coefficients for the multiple diffraction of spherical waves by a series of buildings. *Radio Sci.* **2007**, *42*, 1–15. [[CrossRef](#)]
7. Jay, Y.; Liu, D.; Bird, N.C. Guest Editorial for the Special Issue on Antennas and Propagation Aspects of 60–90 GHz Wireless Communications. *IEEE Trans. Antennas Propag.* **2009**, *57*, 2817–2819.

8. Smulders, P. Exploiting the 60 GHz band for local wireless multimedia access: Prospects and future directions. *IEEE Commun. Mag.* **2002**, *40*, 140–147. [[CrossRef](#)]
9. Smulders, P.; Haibing, Y.; Akkermans, I. On the Design of Low-Cost 60-GHz Radios for Multigigabit-per-Second Transmission over Short Distances [Topics in Radio Communications]. *IEEE Commun. Mag.* **2007**, *45*, 44–51. [[CrossRef](#)]
10. Shay, W.T.; Shen, K.J.; Chen, Y.R.; Lin, Y.Y.; Tsai, Z.M.; Tarnng, J.H. Millimeter-wave channel modelling and ray-tracing method validation. In Proceedings of the 2019 Photonics & Electromagnetics Research Symposium-Fall (PIERS-Fall), Xiamen, China, 17–20 December 2019; pp. 2612–2620.
11. Zhang, P.; Wang, H.; Hong, W. Radio propagation measurement and cluster-based analysis for millimeter-wave cellular systems in dense urban environments. *Front. Inf. Technol. Electron. Eng.* **2021**, *22*, 471–487. [[CrossRef](#)]
12. Wang, H.; Zhang, P.; Li, J.; You, X. Radio propagation and wireless coverage of LSAA-based 5G millimeter-wave mobile communication systems. *China Commun.* **2019**, *16*, 1–18. [[CrossRef](#)]
13. Al-Samman, A.M.; Azmi, M.H.; Al-Gumaei, Y.A.; Al-Hadhrami, T.; Rahman, T.A.; Fazea, Y.; Al-Mqdashi, A. Millimeter Wave Propagation Measurements and Characteristics for 5G System. *Appl. Sci.* **2020**, *10*, 335. [[CrossRef](#)]
14. Uwaechia, A.N.; Mahyuddin, N.M. A Comprehensive Survey on Millimeter Wave Communications for Fifth-Generation Wireless Networks: Feasibility and Challenges. *IEEE Access* **2020**, *8*, 62367–62414. [[CrossRef](#)]
15. Jacob, M.; Priebe, S.; Dickhoff, R.; Kleine-Ostmann, T.; Schrader, T.; Kurner, T. Diffraction in mm and Sub-mm Wave Indoor Propagation Channels. *IEEE Trans. Microw. Theory Tech.* **2012**, *60*, 833–844. [[CrossRef](#)]
16. Kyosti, P.; Carton, L.; Karstensen, A.; Fan, W.; Pedersen, G.F. Frequency dependency of channel parameters in urban LOS scenario for mmwave communications. In Proceedings of the 2016 10th European Conference on Antennas and Propagation (EuCAP), Davos, Switzerland, 10–15 April 2016; pp. 1–5. [[CrossRef](#)]
17. Yamada, W.; Sasaki, M.; Kita, N. Extended Walfisch-Bertoni propagation model to cover short range and millimeter-wave bands. *Radio Sci.* **2021**, *56*, 1–8. [[CrossRef](#)]
18. Kouyoumjian, R.; Pathak, P. A uniform geometrical theory of diffraction for an edge in a perfectly conducting surface. *Proc. IEEE* **1974**, *62*, 1448–1461. [[CrossRef](#)]

Disclaimer/Publisher’s Note: The statements, opinions and data contained in all publications are solely those of the individual author(s) and contributor(s) and not of MDPI and/or the editor(s). MDPI and/or the editor(s) disclaim responsibility for any injury to people or property resulting from any ideas, methods, instructions or products referred to in the content.